Thermally assisted flux flow and melting transition for Mo/Si multilayers

Nina Ya. Fogel, Victoria G. Cherkasova, and Olga A. Koretzkaya

Institute for Low Temperature Physics and Engineering, Kharkov 310164, Ukraine

Anatoly S. Sidorenko*

Physikalishes Institut, Universitat Karlsruhe, Karlsruhe D-76128, Germany

(Received 15 April 1996)

Two-dimensional and three-dimensional vortex-lattice melting is observed for superconducting Mo/Si multilayers. The position of the melting transition on the *H-T* phase diagram is in reasonable quantitative accordance with the existing theories. Above the melting line another phase transition is found connected with the decoupling in the liquid phase or with transition from hexatic to ordinary liquid. The thermally assisted flux-flow (TAFF) regime of the vortex motion is observed in the fluid phase governed by the plastic barrier characteristic for viscous liquid. The TAFF regime with different activation energy takes place also in a vortex solid phase above the depinning line. [S0163-1829(97)02433-2]

New concepts that have appeared in the context of studies of high-T_c superconductivity can be applied for many conventional superconductors, especially for the artificial superlattices (SL's) having the layered structure like their high-T_c counterparts.[1–4] In particular, thermally activated vortex-creep processes, which resemble closely those in high-T_c oxides, were observed on MoGe/Ge,[1] W/Si,[4] and PbTe/PbS (Ref. 3) SL's. On the MoGe/Ge system a decoupling three-dimensional–two-dimensional (3D–2D) phase transition was found,[5] while the vortex lattice melting transition was observed on NbGe/Ge multilayers.[6]

Due to the layered structure and to the essential role of the thermal fluctuations, the *H-T* phase diagram characterizing various states of the vortex ensemble in high-T_c oxides and SL's appeared to be very complicated. This diagram may contain many phases: the regular vortex lattice, vortex glass, vortex liquid, etc. In all of these phases (with the exception of vortex glass) a three-dimensional and a two-dimensional behavior is possible depending on the interlayer coupling strength and on the external magnetic field. The most realistic way to investigate a large variety of the interesting phenomena mentioned is to use artificial superconducting SL's where the layer thicknesses and interlayer coupling may be changed in an arbitrary way.

Here, for Mo/Si multilayers, we investigate the different regimes of thermally activated dissipation at the vortex motion in the magnetic fields orthogonal to the layers. Observation of the specific features of the Arrhenius plots allows us to determine the vortex-lattice melting transition line. Three-dimensional melting occurs in the weak-field range, while in the higher magnetic fields the crossover to quasi-two-dimensional melting takes place. The positions of both 3D and quasi-2D melting lines agree quantitatively with the theoretical predictions. The thermally assisted flux-flow (TAFF) regime is observed above the melting line as well as below it. The TAFF activation energy dependence on *H* and *T* is obtained. In the vortex liquid phase this dependence corresponds to the plastic vortex line motion, charasteristic for viscous or entangled liquid. Above the melting transition another transition occurs which may be identified as the transition between hexatic and ordinary vortex liquid or as decoupling transition in the liquid phase. The correlations between phase transition line positions and activation energies for vortex motion are established.

The measurements have been carried out on Mo/Si SL's with 30–50 bilayers prepared by magnetron sputtering. The thickness of Mo layers have been varied in the range 22-35 Å, and Si layers have been varied in the range 34–66 Å. The sample preparation and characterization were described in Ref. 7. Both Mo and Si layers were amorphous. A standard low-frequency ac technique was used for measurements of resistance on the samples with four-probe geometry. The accuracy of temperature measurements was ∼1 mK, the stabilization of magnetic field was about 0.1% from the value chosen.

The resistive transitions in magnetic fields are broadened in the same manner as on high-T_c compounds. The Arrhenius plots demonstrating thermally activated resistivity behavior in perpendicular fields are shown in Fig. 1. For all samples investigated two clearly defined temperature ranges
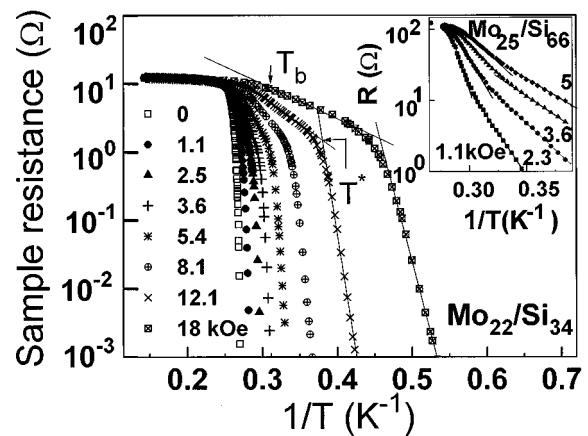
FIG. 1. Arrhenius plots of the resistance of two Mo/Si SL's. Arrows in the main panel show the way of T^* and T_b determination.
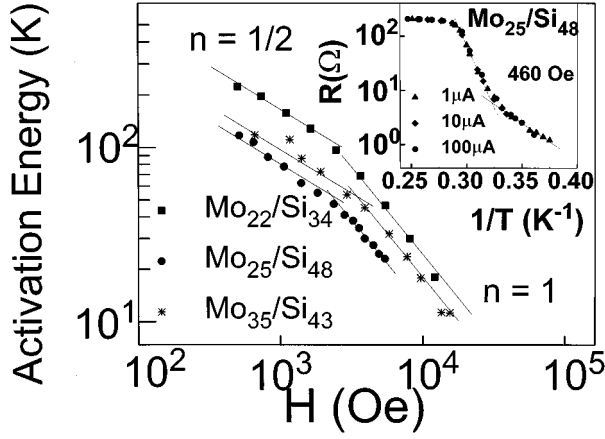
FIG. 2. Dependences of the activation energy U_A on magnetic field for three samples. Inset: Arrhenius plot for different currents for one of the SL's.

FIG. 3. H-T phase diagrams for two Mo/Si SL's. Lines 1 correspond to the temperature $T^*(H)$, lines 2 correspond to temperature $T_b(H)$. Filled symbols are the experimental data. Solid curves are the fits to Eq. (4). The procedure of fitting is described in the text. Dashed lines represent equations $U_A(H,T)=kT$ and $U_B(H,T)=kT$. Dotted-dashed line on the upper panel is a fit to Eq. (5). Crosses represent dependence $T_p(H)$.

may be singled out on these plots where $\ln R$ is linear with T^{-1}, but with different slope. These two regions (A and B, respectively) for one of the curves are shown in Fig. 1 with two solid lines. There are two types of Arrhenius plot behavior: for some SL's at lower temperatures (larger T^{-1}, part B) the activation energy U_B is higher than at temperatures close to T_c (Fig. 1), for other samples the opposite situation is observed (inset in Fig. 1). Typical dependences of the activation energy on magnetic field are shown in Fig. 2. All these curves that are related to the parts A of Arrhenius plots behave in the similar way. In the weak-field range $U \sim H^{-1/2}$, and in strong fields $U \sim H^{-1}$. The inset in Fig. 2 demonstrates one of Arrhenius plots obtained with different transport currents ranging from 1 to 100 μA. The same behavior is observed at all H values. From these data one may conclude that in the two orders of j variation the activation energy is independent of current and, respectively, thermally activated flux flow (TAFF) takes place. This statement is valid for both A and B ranges of the resistive transitions.

Both U_A and U_B change linearly with (T_c-T), and a common formula for the both regimes looks like

$$U_{A,B} = U_{0A,B}(1-T/T_c)/H^n \qquad (1)$$

with an exponent $n=1/2$ or 1. For high-T_c oxides both types of U vs H dependence were observed also (see Ref. 3 and references therein). There are two characteristic temperatures on all Arrhenius plots, T^* and T_b. One of them, T^*, separates two regimes of thermally activated resistance behavior. Another one, T_b, corresponds to the transition from TAFF to slower R change with T, characteristic for a viscous flux-flow regime. These temperatures as a function of H are shown for two SL's in Fig. 3. Both lines, $T^*(H)$ and $T_b(H)$ terminate at the strong-field range by about vertical portions. Such behavior implies that these lines may be associated with a melting transition, their vertical parts defining the temperature of quasi-2D melting.

It is known[8] that the temperature of quasi-2D melting in layered superconductors is close to the temperature of authentic 2D vortex lattice melting in the case of the weak interlayer coupling or, equivalently, in the case of suffi-

ciently high magnetic field $H \gg H_0$. A characteristic magnetic field H_0, where crossover from 3D to 2D vortex fluctuations takes place, is defined as[9]

$$H_0 = \alpha \Phi_0 / \gamma^2 s^2. \qquad (2)$$

Here s is an interlayer distance, $\gamma = (M/m)^{1/2}$ is an anisotropy parameter, α is a numerical factor. A genuine 2D melting temperature is[8,10]

$$kT_m^{2D} = \frac{A\Phi_0^2 d}{256\pi^3\lambda^2(T_m^{2D})} = \frac{A\Phi_0^2}{128\pi^3\lambda_\perp(T_m^{2D})}. \qquad (3)$$

Here Φ_0 is the magnetic flux quantum, λ is the London penetration depth, $\lambda_\perp = 2\lambda^2/d$ is an effective penetration depth, d is the film thickness, A is the numerical factor whose value has to be 0.4–0.7.[10] A weak dependence of quasi-2D melting temperature on H in strong-field range[8,11] enables one to compare vertical parts of lines 1 and 2 in Fig. 3 with formula (3). The single parameter defining temperature T_m^{2D} is $\lambda_\perp$. Its value for all samples may be determined through the sheet resistance $R_\square$, using the known relation[12] $\lambda_\perp(0) = 0.83 \times 10^{-4} R_\square/T_c$. ($\lambda$ is in cm, R in Ω, T_c in K.) Since parameter A in Eq. (3) is not known precisely, the most convenient way to compare the experimental values of T_m^{2D} with formula (3) is to find A values and to determine whether the A's for different samples are close one to another and to the cited above value $A=0.4$–0.7. In such a procedure one does not need any fitting parameters. In formula (3) the temperature dependence of $\lambda_\perp \sim (T_c-T)^{-1}$ near T_c is used. The A values obtained for different multilayers from comparison of the experimental data for lines 1 on the phase diagrams with formula (3) are listed in Table I. For three samples $A \sim 0.3$ is obtained in a rather good agree-

TABLE I. The samples and their derived parameters.

Sample d_{Mo}/d_{Si} (Å) (Å)	T_c (K)	$\lambda_\perp(0)$ (10^{-4} cm)	T_M^{2D} (K)	A	γ	c_L
25/66	3.57	7.8	3.23	0.33	10.3	0.23
25/48	3.42	9.2	3.02	0.30	13.1	0.21
22/43	4.26	3.3	4.05	0.35	16.7	
35/43	4.29	7.2	3.17	0.11	10.0	0.17
				(0.29 [a])		

[a]The value $A=0.29$ for Mo_{35}/Si_{43} is obtained for line 2 of the H-T phase diagram.

ment with the theoretical prediction. For sample Mo_{35}/Si_{43} the value $A=0.29$ is obtained for line 2.

In weak magnetic fields the theory[8,11] predicts 3D melting with a melting temperature T_m^{3D} depending on H:

$$kT_m^{3D} = \frac{c_L^2 \Phi_0^{5/2}}{4\pi^2 (M/m)^{1/2} H^{1/2} \lambda^2(T_m^{3D})}. \quad (4)$$

Here c_L is a Lindemann number which is assumed to be 0.1–0.2.[8] The fitting of lines 1 and 2 on H-T phase diagrams with this formula is shown as a solid line. The coefficient c_L^2/γ is used as a fitting parameter. The functional form of Eq. (4) is in a good agreement with the experimental data. The quantitative comparison may be carried out if the γ's are known. Having now no data about γ, one can proceed in such a way. For all samples there is a characteristic magnetic field where the activation energy for TAFF changes its dependence on H (Fig. 2). Assuming this change takes place at the field H_0, one may define γ's for all SL's (Ref. 13) from formula (2), putting $\alpha=1$, with a precision up to some numerical factor and determine the values of c_L (Table I). As in the case of T_m^{2D}, for three samples c_L values defined from lines 1 are close to one another and close to the expected value $c_L=0.2$.

Summarizing this part of the discussion one may conclude that line 1 on the H-T diagram reflects 3D and quasi-2D melting. From measurements of I-V curves in magnetic fields it follows that depinning temperature T_p where the critical current disappears (Fig. 3) is close to line 1. This means that pinning becomes ineffective at melting transition as may be expected due to the absence of the long-range order in the vortex liquid.[14] This gives additional evidence that line 1 is reasonably considered as the melting transition.

As for line 2 on H-T diagrams, different possibilities to explain their origin may be considered. It may be a boundary between hexatic and ordinary isotropic liquid.[10] Another explanation of line 2 may be associated with the predicted transition between a liquid of vortex lines and the independent liquid systems of 2D vortices in different layers.[11] The form of this transition line is[11]

$$\widetilde{H}_m(T) = \frac{\alpha_m \Phi_0^3}{16\pi^3 kT \lambda^2(T) (M/m)^{1/2}}. \quad (5)$$

Here α_m is universal constant. Fitting of the experimental data with formula (5) is presented in Fig. 3.

In the weak-field range the experimental dependence $U_A(T,H)$ is consistent with the expansion for the plastic barrier in the viscous vortex liquid

$$U_{pl} \sim \frac{(m/M)^{1/2} \Phi_0^2 a_0}{8\pi^2 \lambda^2} = \frac{\Phi_0^{5/2}}{8\pi^2 \lambda^2 (M/m)^{1/2} H^{1/2}} \sim \frac{(1-t)}{H^{1/2}} \quad (6)$$

proposed in Ref. 14. Here a_0 is an intervortex distance. This formula characterizes the TAFF regime of the viscous vortex liquid. In the case of the plastic motion of vortices in the liquid phase there should not be dependence of U_{pl} on transport current,[14] and this corresponds to experiments (Fig. 2). Thus between lines 1 and 2 in the weak-field range the vortex motion corresponds to the TAFF regime of the viscous vortex liquid. The change of the exponent in the U_A vs H dependence at $H>H_0$ may be a consequence of another dissipation mechanism in a quasi-2D situation.

The melting transition line 1 separates the vortex liquid from the vortex lattice phase. Because strong $U(j)$ dependence characteristic for vortex glass is absent in the area below line 1, this line cannot be associated with glass transition. The transition between vortex liquid and vortex-lattice phases was observed in experiments[15] on Y-Ba-Cu-O crystals.

At $T<T^*$ the dependence $U_B(T,H)$ for the vortex lattice is the same as in the vortex liquid. This type of dependence with energy barrier $U_c \sim C_{66} a_0^3 \sim (1-t)/H^{1/2}$ for vortex bundle creep may be obtained on the basis of the results[15–18] in the case of the collective pinning under definite assumptions about the pinning volume V_c, which are discussed in detail elsewhere. Formula (6) for U_{pl} contains as a factor the anisotropy parameter. Depending on its value, U_c may be less or larger than U_{pl}. Thus resistivity behavior at $T<T^*$ can be interpreted as a collective creep of the vortex bundles. However, the reason for the U_c insensitivity to j in the solid phase is not clear.

It is important also to mention that some correlation between $U_{A,B}(T,H)$ and the position of the phase transition lines on the H-T diagram exists. Two dashed curves in Fig. 3, $T_A'(H)$ and $T_B'(H)$, mark the values of H corresponding to the condition $U_{pl}=U_A(H,T)=kT$ at which the transition from TAFF to vortex flow should occur[14] and to condition $U_B(H,T)=kT$. The agreement between the curve $T_B'(H)$ and line 1 for Mo_{25}/Si_{66} is rather good, especially if one takes into account that no fitting parameters were used. The curve $T_A'(H)$ is similar in its shape to line 2 in the weak-field range, but lies somewhat below it. Excellent agreement between the boundary $U_{pl}(H,T)=kT$ and line 2 is obtained in the range of 3D behavior for Mo_{35}/Si_{43}. Thus in some cases line 2 may be associated with a transition to viscous flux flow.

In summary, we have shown that the vortex-lattice melting transition is observed on the artificial Mo/Si multilayers. This transition is three-dimensional in the weak-field range and quasi-two-dimensional in high fields. For a number of Mo/Si samples rather good agreement with the theory of melting[9–11] is obtained. In particular, the Lindemann number $c_L=0.2$ is obtained in agreement with standard melting criterion. The temperature of quasi-2D melting is also consistent with the predictions.[9–11] 3D–2D crossover in melting is

associated with the decoupling of vortices in the adjacent layers which takes place at fields $H > H_0$. This type of decoupling does not exclude another decoupling transition in the weak-field range at higher temperatures. The data on 3D–2D crossover differ from those obtained on NbGe/Ge SL's (Ref. 6) because in the latter case crossover is connected with the finite-size effect. Along with melting transition another line on the H-T phase diagram is found which can be interpreted as a transition between hexatic and ordinary vortex liquids or as a decoupling transition. In some cases this line coincides with a crossover from the TAFF regime to the viscous flux flow. Two different TAFF regimes are observed. It is shown that the activation energy controlling the TAFF regime in viscous liquid is associated with the plastic motion of the vortices with plastic barrier $U_{\text{pl}} \sim (m/M)^{1/2} \Phi_0^2 a_0 / (8\pi^2 \lambda^2)$ in accordance with theory.[14]

---

*Permanent address: Institute of Applied Physics, Kishinev, 277028 Moldova.

[1] W. R. White, A. Kapitulnik, and M. R. Beasley, Phys. Rev. Lett. **66**, 2826 (1991).

[2] M. F. Schmidt, N. E. Israeloff, and A. M. Goldman, Phys. Rev. B **48**, 3404 (1993).

[3] N. Ya. Fogel, V. G. Cherkasova, A. Yu. Sipatov, A. I. Fedorenko, and V. N. Rybalchenko, Fiz. Nizk. Temp. **20**, 1142 (1994) [Low Temp. Phys. **20**, 897 (1994)].

[4] E. Majkova, S. Luby, M. Jergel, H. v. Lohneysen, C. Strunk, and B. George, Physica Status Solidi A **145**, 509 (1994).

[5] D. G. Steel, W. R. White, and J. M. Graybeal, Phys. Rev. Lett. **71**, 161 (1993).

[6] P. Koorevaar, P. H. Kes, A. E. Koshelev, and J. Aarts, Phys. Rev. Lett. **72**, 3250 (1994).

[7] E. I. Buchstab, V. Yu. Kashirin, N. Ya. Fogel, V. G. Cherkasova, V. V. Kondratenko, A. I. Fedorenko, and S. A. Yulin, Fiz. Nizk. Temp. **19**, 704 (1993) [Low Temp. Phys. **19**, 506 (1993)].

[8] M. V. Feigel'man, V. B. Geshkenbein, and A. I. Larkin, Physica C **167**, 177 (1990).

[9] V. M. Vinokur, P. H. Kes, and A. E. Koshelev, Physica C **168**, 29 (1990).

[10] D. S. Fisher, Phys. Rev. B **22**, 1190 (1980).

[11] L. I. Glazman and A. E. Koshelev, Phys. Rev. B **43**, 2835 (1991).

[12] K. K. Likharev, Izv. Vyssh. Uchebn. Zaved. Radiofiz. **14**, 919 (1971).

[13] The estimated value of γ for Mo_{25}/Si_{66} is less than one for the sample Mo_{25}/Si_{48} with the thinner Si layers. This seeming inconsistency is connected with anomalous oscillating behavior of the anisotropy parameter on Mo/Si SL's [N. Ya. Fogel, O. G. Turutanov, A. S. Sidorenko, and E. I. Buchstab (unpublished)] which correlates with quantum size oscillations of normal resistivity and superconducting parameters (T_c, dH_{c2}/dT) found on the SL's investigated (see Ref. 7).

[14] V. M. Vinokur, M. V. Feigel'man, V. B. Geshkenbein, and A. I. Larkin, Phys. Rev. Lett. **65**, 259 (1990).

[15] T. K. Worthington, M. P. A. Fisher, D. A. Huse, J. Toner, A. D. Marwick, T. Zabel, and F. Holtzberg, Phys. Rev. B **46**, 11 854 (1992).

[16] M. V. Feigel'man, V. B. Geshkenbein, A. I. Larkin, and V. M. Vinokur, Phys. Rev. Lett. **63**, 2303 (1989).

[17] P. H. Kes, J. Aarts, J. van den Berg, C. J. van der Beek, and J. A. Mydosh, Supercond. Sci. Technol. **1**, 242 (1989).

[18] R. Wordenweber and P. H. Kes, Phys. Rev. B **34**, 494 (1986).